Developmental Biology 340 (2010) 170–178

Contents lists available at ScienceDirect

Developmental Biology

journal homepage: www.elsevier.com/developmentalbiology

Review

The gene regulatory network basis of the "community effect," and analysis of a sea urchin embryo example ☆

Hamid Bolouri, Eric H. Davidson *

Division of Biology, California Institute of Technology, Pasadena, CA 91125, USA

ARTICLE INFO

Article history:
Received for publication 18 March 2009
Revised 20 May 2009
Accepted 5 June 2009
Available online 10 June 2009
doi:10.1016/j.ydbio.2009.06.007

Keywords:
Community effect
Intradomain signaling
Sea urchin embryo
nodal gene regulation

ABSTRACT

The "Community Effect" denotes intra-territorial signaling amongst cells which constitute a particular tissue or embryonic progenitor field. The cells of the territory express the same transcriptional regulatory state, and the intra-territorial signaling is essential to maintenance of this specific regulatory state. The structure of the underlying gene regulatory network (GRN) subcircuitry explains the genomically wired mechanism by which community effect signaling is linked to the continuing transcriptional generation of the territorial regulatory state. A clear example is afforded by the oral ectoderm GRN of the sea urchin embryo where *cis*-regulatory evidence, experimental embryology, and network analysis combine to provide a complete picture. We review this example and consider less well known but similar cases in other developing systems where the same subcircuit GRN topology is present. To resolve mechanistic issues that arise in considering how community effect signaling could operate to produce its observed effects, we construct and analyze the behavior of a quantitative model of community effect signaling in the sea urchin embryo oral ectoderm. Community effect network topology could constitute part of the genomic regulatory code that defines transcriptional function in multicellular tissues composed of cells in contact, and hence may have arisen as a metazoan developmental strategy.

Introduction

John Gurdon introduced the term "Community Effect" to describe the requirement for continuing contact among prospective dorsal mesoderm cells of *Xenopus* embryos for muscle-specific actin expression, in response to induction from vegetal cells. Single animal cells sandwiched between vegetal cell masses or scattered monolayers failed to express muscle actin a day later while virtually every cell in 3-dimensional aggregates surrounded by the inducing vegetal cells did so. The result implied some form of signaling among the responding cells (Gurdon, 1988). Twenty years on, it appears that signaling within a developmental territory which proves necessary for the maintenance of the specific territorial regulatory state, is probably a very widespread phenomenon (Davidson, 2006). Indeed intra-territorial community effect signaling is perhaps just as widespread as is inductive inter-territorial signaling, though it has thus far been relatively little considered.

As the structure/function relations of developmental gene regulatory networks (GRNs) have come into focus, the genomically encoded wiring that causally underlies many aspects of developmental phenomenology are becoming resolved. Among such phenomena that we now understand better is community effect signaling. Study of the relevant GRNs reveals an elemental, common form of subcircuit which in known cases is directly responsible for this type of signaling (Davidson, 2006). This is shown abstractly in Fig. 1A. The definitive feature is that transcription of the gene encoding the community effect signaling ligand is directly dependent on that signal transduction system which is activated in cells receiving the signal. Thus adjacent cells receiving a short range signal emit the ligand, but also receive it, the result of which is continuing mutual activation of transcription of the ligand gene: all cells of the territory are locked in a positive feedback regulatory embrace in which the given signal transduction system is activated, leading to common activation of responsive downstream genes. In contrast (Fig. 1B), in inductive signaling, the signal emitting and signal receiving cells express different regulatory states, the first used to cause ligand expression; the second installed in response to reception of the signal.

Here we review in some detail how a relatively well known example of community effect signaling encountered in the GRN of the sea urchin embryo actually works. Other cases from other systems are briefly reviewed. We then illuminate with the aid of a quantitative model some aspects of community effect mechanism which are not immediately obvious. Among the issues we address are whether community effect signaling could impose uniformity in the intensity of regulatory state expression in the cells of a territory; and how the transcriptional feedback mechanism is controlled quantitatively. We conclude by considering community effect signaling in an evolutionary light, since it could be a defining mechanism of tissues composed of similarly functioning cells in architectural contact with one another.

☆ This article was accepted in 2009 to celebrate the 50th anniversary of Developmental Biology.

* Corresponding author. Fax: +1 626 793 3047.
E-mail address: Davidson@caltech.edu (E.H. Davidson).

0012-1606/$ – see front matter © 2009 Elsevier Inc. All rights reserved.
doi:10.1016/j.ydbio.2009.06.007

An example: the *nodal* community effect in the sea urchin embryo oral ectoderm

Expression of the *nodal* gene, which encodes a TGFβ family signaling ligand, is the earliest known transcriptional event in the specification of the oral ectoderm (Duboc et al., 2004; Flowers et al., 2004). In *S. purpuratus nodal* transcription is activated by 5th cleavage, the first stage at which founder cell lineages for oral vs aboral ectoderm have separated according to lineage tracing data (Cameron et al., 1990). By hatching blastula stage the domain of *nodal* expression delimits the "facial" oral ectoderm as seen in the vegetal view of a *nodal* WMISH (Fig. 2A), and excludes both the apical and endomesodermal vegetal domains as seen in the lateral view. Duboc et al. (2004, 2008) showed by morpholino antisense oligonucleotide (MASO) treatment that *nodal* expression is directly required for specification of oral territories, and indirectly for correct delimitation and specification of the aboral territories as well. These studies also showed that later expression of the oral ectoderm regulatory genes *brachyury* (*bra*) and *goosecoid* (*gsc*) is abolished by *nodal* MASO. Thus *nodal* expression within the oral ectoderm appeared necessary for the expression of the downstream oral ectoderm regulatory state. With the construction of a large scale gene regulatory network (GRN) for oral and aboral ectoderm specification (Su et al., 2009) the central role of *nodal* in the generation of the oral ectoderm regulatory state became explicit. The network downstream of *nodal* is not our subject here; suffice it to say that the immediate regulatory targets of the Smad2/3 transcription factor phosphorylated in sea urchin embryos by reception of the nodal signal (Yaguchi et al., 2007), are two regulatory genes, *gsc* and *foxg*. About a dozen other transcriptional regulatory genes (including *bra*) are activated very specifically in the oral ectoderm or subdomains thereof, prior to gastrulation, downstream either of *gsc* and *foxg*, or of a second independent regulatory pathway, or both. The architecture of the oral ectoderm GRN explains completely the disastrous effects on oral ectoderm specification of blocking *nodal* mRNA translation, as many downstream regulatory genes fail to be expressed and the oral ectoderm regulatory state is never constructed.

Expression of the *nodal* gene in the cells of the same territory where its signal transduction system is utilized to generate and maintain the territorial regulatory state identifies a case of the community effect, *prima facie*. The regulatory key to the operation of the community effect was predicted to be the subcircuit topology shown in Fig. 1A, which here would require that the *nodal* gene is positively regulated by the phosphorylated Smad2/3 factor in cells receiving the Nodal signal. The receptor for the Nodal ligand is Alk4, as shown by Yaguchi et al. (2007), who also demonstrated by ectopic expression that the Nodal signal does not cause activation of Smad2/3 more than one or two cell diameters away from the cells in which *nodal* mRNA is being translated. All cells in the oral ectoderm where *nodal* is expressed should express the *nodal* gene driven by reception of the Nodal signal from the next-door cells (and perhaps from themselves as well), in addition they should express the immediately downstream *gsc* and *foxg* genes. The genome level prediction is that the activity of the *nodal cis*-regulatory system should be dependent on the presence of Nodal, and that it should include Smad target sites which are required for normal expression. These predictions were tested and verified in a *nodal cis*-regulatory study by Nam et al. (2007), and have been independently supported in a second *cis*-regulatory study as well (Range et al., 2007). Some of the evidence demonstrating the crucial feedback onto the *nodal cis*-regulatory system of the Nodal signal transduction input, from the experiments of Nam et al. (2007) is reproduced in Fig. 2B.

Part 1 of Fig. 2B shows the map of the relevant portions of the *nodal cis*-regulatory system, consisting of two interspecifically conserved *cis*-regulatory modules, one upstream (5P) and one in an intron (INT). The reporter contains a GFP sequence knocked into the sequence of exon1. Expression constructs containing either or both of these modules produce specific oral ectoderm expression (Nam et al., 2007). Parts 2 and 3 of Fig. 2B demonstrate that the short 5P and INT constructs depend strongly on Nodal translation for their expression, as the major part of their transcriptional output is abolished by treatment with *nodal* MASO. This relationship is a direct one, as shown in part 4 of Fig. 2B, and by extensive further evidence in Nam et al. (2007) and Range et al. (2007): mutation of the *nodal cis*-regulatory Smad sites has the same effect as does interference with the *trans* input to these sites, i.e., blocking Nodal translation. The *nodal cis*-regulatory feedback of course cannot be responsible for turning on the gene in the oral ectoderm in the first place. This function is executed via sites for b-zip factors (Nam et al., 2007; Range et al., 2007), the activity of which may reflect the oral/aboral redox polarity initially responsible for distinguishing the oral from aboral domains in early cleavage (Coffman and Davidson, 2001; Coffman et al. 2004), plus a boost from an input downstream of a maternal signaling ligand, Univin (Range et al., 2007).

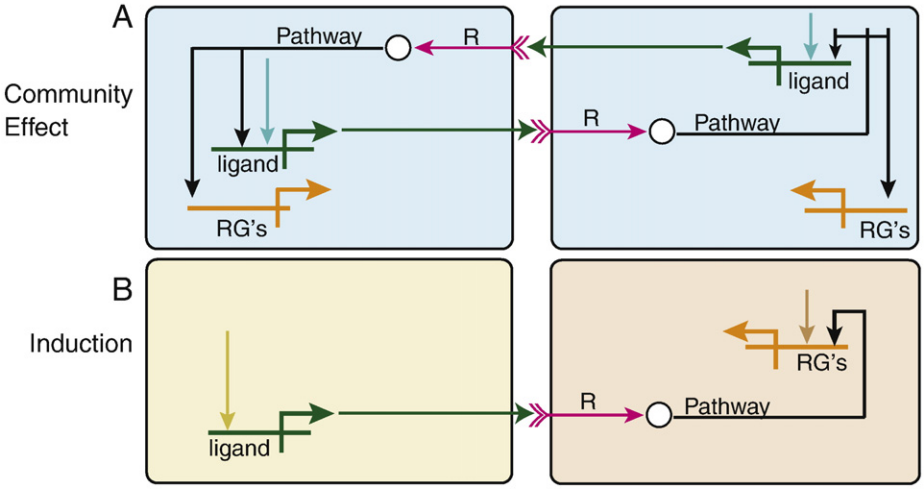

Fig. 1. Abstract diagram of subcircuit hypothesized to underlie community effect and canonical inductive signaling. (A) Community effect signaling. Two cells of the many constituting the field within which the community effect obtains are shown. Each expresses the signaling ligand gene (green) which activates a signal transduction pathway (black) following binding to the receptor (double arrow tail). The result is feedback activation of the gene encoding the ligand, which also receives an independent initial input (blue arrow). The same downstream regulatory genes (RG's, orange), are consequently activated in both cells. (B) Inductive signaling. The cell expressing the ligand gene and the cell receiving the signal have different regulatory states, specifically because in the receiving cell the signal transduction results in activation of regulatory gene(s) not expressed in the sending cell, while the receiving cell does not express the ligand gene.

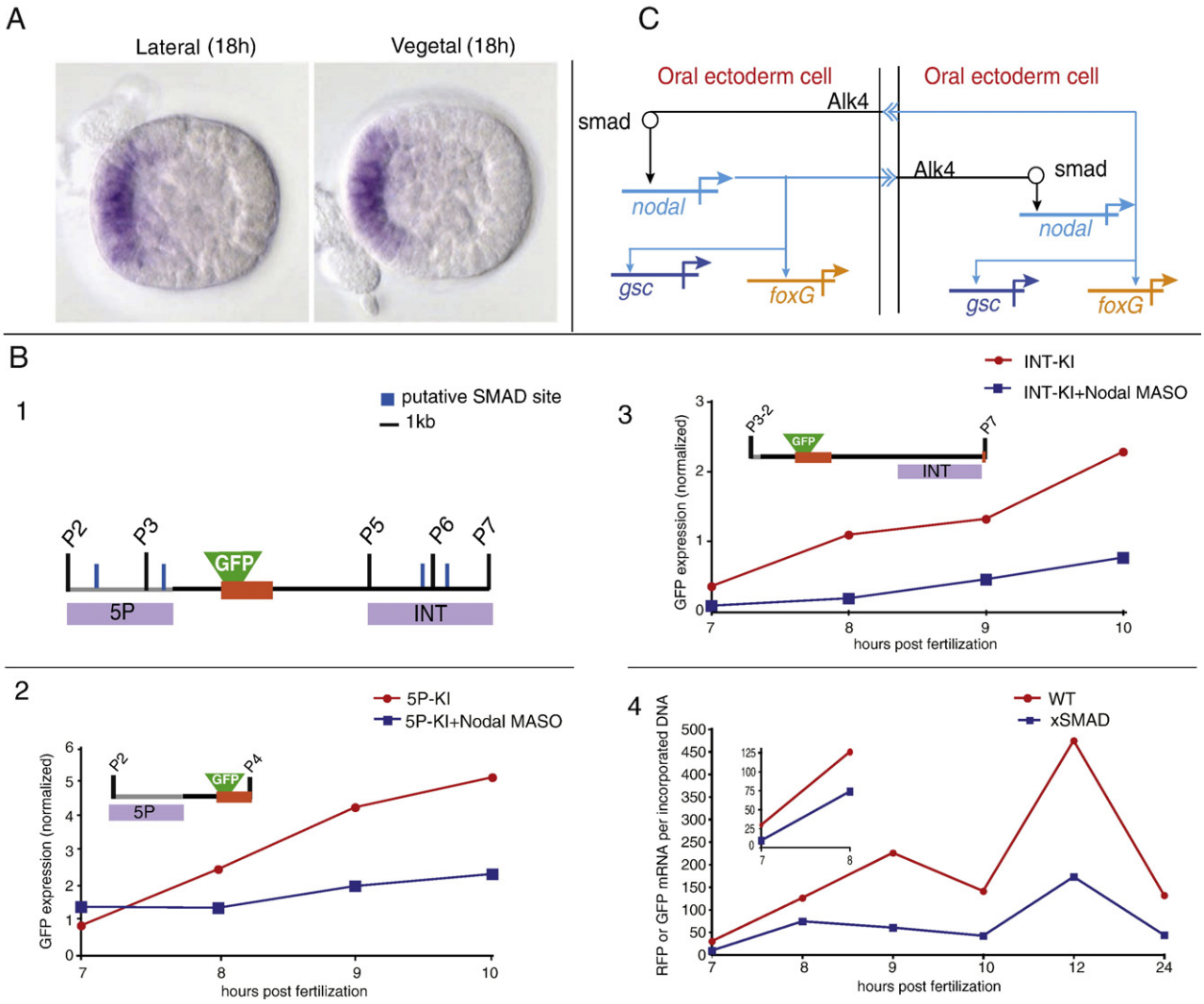

Fig. 2. The sea urchin oral ectoderm *nodal* community effect: *cis*-regulatory evidence. (A) *nodal* expression domain. WMISH images made at 18 h are shown viewed from the lateral (left) and vegetal aspects so as to reveal boundaries of expression. (B) *Cis*-regulatory evidence. Data are from Nam et al. (2007) where many additional experiments are also to be found; see also Range et al. (2007). (1) Map of *nodal cis*-regulatory domain displaying an upstream (5P) and an intron (INT) module; a GFP coding sequence (green) has been knocked into the first exon of the gene (red). (2) Quantitative expression of GFP mRNA above background generated by 5P construct, monitored by QPCR, is >80% abolished by *nodal* MASO. (3) A similar result is obtained with INT construct. (4) Mutation of Smad sites in construct shown in Part 1 (two sites each in 5P and INT) greatly reduces activity by abolishing feedback, though there is little effect on initial rate of output (inset). (C) Upstream GRN subcircuit including community effect linkage and immediately downstream genes. Network data from Su et al. (2009).

The wiring of the subnetwork in Fig. 2C is thus supported directly by *cis*-regulatory evidence, together with the demonstration that Nodal signal transduction in sea urchin embryos occurs via the Alk4–Smad2/3 pathway (Yaguchi et al. (2007), and the GRN analysis of Su et al. (2009). Nodal signaling within the oral ectoderm territory has two consequences illustrated in this subcircuit: intercellular feedback promoting continued *nodal* gene expression in all cells of the territory; and continuing transcriptional activation of the downstream target genes, *gsc* and *foxg*, which initiate the oral ectoderm regulatory state.

Other examples

Are there other examples of genes encoding peptide signaling ligands which are expressed within territories, and which have been demonstrated to respond to the transcriptional inputs activated by reception of their own signal transduction systems? Following are some relevant cases:

- In ventrolateral regions of the *Xenopus* embryo, BMP4 is expressed. The immediate early response factor transducing this signal is Oaz, which provides an input into the *vent2b* gene, expressed in the same domain. But *vent2b* together with other factors also provides a direct *cis*-regulatory input into the gene encoding the Bmp4 ligand in the same domain (reviewed by Koide et al. (2005); Cao et al. (2006)).
- eFGF is also expressed in the *Xenopus* embryo and its signal transduction system activates the *bra* gene; *cis*-regulatory analysis shows that Bra in turn provides a positive input to the gene encoding the eFGF ligand (reviewed by Koide et al. (2005)).
- In the sea urchin endomesoderm, the *wnt8* gene is expressed, and both *cis*-regulatory and *trans* perturbation evidence shows that this gene requires for its continued expression the Tcf/βcatenin input that is generated by reception of the Wnt8 signal within the same territory (Minokawa et al., 2005; Smith et al., 2007).
- In *Drosophila*, the gene encoding the Dpp Tgfβ ligand has been shown to be autoregulated in response to its own signal in several domains of its expression: in the midgut visceral mesoderm (Hursh et al., 1993; Staehling-Hampton and Hoffmann, 1994); in the eye disc (Chanut and Heberlein, 1997); in the wing disc (Hepker et al., 1999).

- In zebrafish, maintenance of ventral expression of Bmp2b depends directly on smad5, the transcription factor that mediates Bmp2b signaling via the Alk8 receptor (Bauer et al., 2001; Hild et al., 1999).

While pertinent *cis*-regulatory evidence is limited, there is another kind of experiment that was widely done in earlier times, the results of which could imply the general existence of community effects. These were disaggregation and culture experiments, in which it was observed that cell type specific function or character is lost in culture soon after cells become separated from one another. In a canonical example from the early 1980's, the consequences of disaggregation of liver were measured with liver-specific and non-specific probes using RNA gel blots (Clayton and Darnell, 1983; Clayton et al., 1985). Strikingly, transcription of liver-specific genes decreased beginning after only 2–4 h in culture, and thereafter almost disappeared, while transcription of generally expressed genes remained constant for days or in some cases increased. Or, put another way, these experiments showed that maintenance of the liver-specific regulatory state requires continuous cell interaction. Community effect signaling and wiring analogous to that in Fig. 2C would explain such results, though in this case the nature of the intercellular interaction has never been discovered.

The majority of the examples of ligand gene *cis*-regulatory systems that respond to their own signal transduction systems listed above concern members of the Tgfβ family of signaling ligands. However, note that there is at least one example from an entirely different signaling system which has been thoroughly authenticated at the *cis*-regulatory level, that of the sea urchin *wnt8* gene (Minokawa et al., 2005; Smith et al., 2007). Therefore this wiring topology is not confined to Tgfβ genes. In addition the *Xenopus efgf* gene lies in a similar subcircuit, though as noted above, the signal transduction system here results in activation of a gene encoding a transcription factor (*brachyury*), which in turn activates the *efgf* gene, one step removed from a direct interaction. Nor is this type of subcircuit confined to deuterostomes, although most of the cases we have are of that superclade (the sea urchin and vertebrate cases). The several *Drosophila dpp* gene *cis*-regulatory modules also operate in this manner (see above). Thus we may conclude that intercellular community effect autoregulatory wiring could be a trans-bilaterian regulatory feature for genes encoding Tgfβ ligands, and to an unknown extent the same wiring occurs in other signaling ligand families as well.

A model reproducing mechanistic aspects of the nodal community effect in the sea urchin oral ectoderm

A puzzling feature of the subcircuit in Fig. 2C emerges on consideration of its kinetic and quantitative implications: what keeps the rate of *nodal* transcription from continuously accelerating, and the amount of *nodal* mRNA and protein from continuously increasing in response to the continuing positive feedback built into this system? Direct measurements of endogenous *nodal* mRNA show that over the 24 h period postfertilization the quantity of transcript attains a steady state plateau rather than increasing continuously (Nam et al., 2007). This is not due to saturation of transcription rate at the maximum level (cf Bolouri and Davidson, 2003), since as we show below the rate of *nodal* gene transcription is only a few percent of the maximum. A qualitative study of Duboc et al. (2008) confirmed that in sea urchins as in vertebrates the Nodal antagonist Lefty is expressed together with nodal. This protein evidently diffuses faster than Nodal and Duboc et al. (2008) showed that it is responsible for blocking the spatial spread of Nodal beyond the boundary of the oral ectoderm. Su et al. (2009) found that the *lefty* gene is another immediate downstream target of community effect *nodal* signaling within the oral ectoderm, and thus it is expressed in the same cells as express the *nodal* gene, beginning soon after *nodal* expression (Duboc et al., 2008; Su et al., 2009). Lefty is thus a possible candidate for the function of maintaining a constant level of *nodal* mRNA, by binding to Nodal (and also the Alk4 receptor; Chen and Shen, 2004; Cheng et al., 2004: Hild et al., 1999; Sakuma et al., 2002) and thus damping the amplitude of the *cis*-regulatory feedback onto the *nodal* gene. Since *lefty* is expressed under transcriptional control of the same activated Smad that is generated by reception of the Nodal signal, the implication is that there must be a negative as well as positive feedback for the community effect subcircuit to work. To explore this qualitative idea, and determine if it indeed generates the observed behavior using kinetic parameters estimated from measurements, we built the model described in the following. The observed behavior to be tested against the model should include the consequences of blocking expression of one or another of the components of the subcircuit by MASO treatment. A further objective was to ask (in silico) whether community effect signaling could have the function of smoothing out any local cell by cell fluctuations in the intensity of expression of the regulatory state, as one might intuitively suppose.

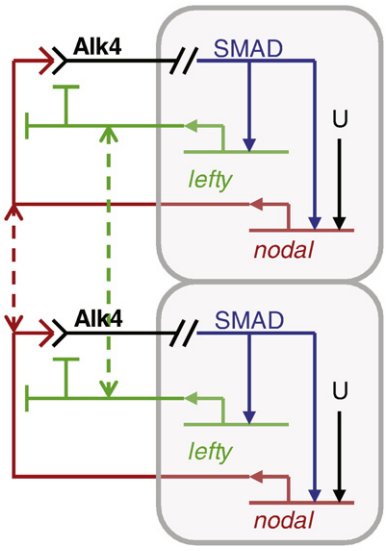

Fig. 3. Lefty–Nodal community effect interactions modeled. For simplicity only two cells within the community effect zone are shown (rounded rectangles). Inter-cellular diffusion of Nodal and Lefty protein molecules is indicated by dashed arrows. Within each cell, the horizontal lines crossed by a right-angle arrow indicate a gene (*nodal* and *lefty* as labeled). Arrows incident onto each gene indicate transcriptional activation by the indicated factor. Zygotic transcription of the *nodal* gene is initiated jointly by the ubiquitous activator Univin (Range et al., 2007) and a redox-sensitive b-zip factor (Nam et al., 2007; Range et al., 2007). As discussed previously (Bolouri and Davidson, 2002), the level of activity of the initial signal need not be uniform across all cells in the region. Any cells in the zone that are short of or lacking in the initial signal will be activated by the diffusion of Nodal ligands from other cells. Nodal:Alk4 dimerization results in phosphorylation of SMAD2/3, which then translocates to the nucleus and acts as a transcriptional activator of both *nodal* and *lefty* (Su et al., 2009; Nam et al., 2007). Lefty molecules can dimerize with both Nodal, and its receptor Alk4 and thereby disrupt Nodal:Alk4 dimerization (indicated by the lines ending in bars).

The interactions and processes represented in the model are shown in Fig. 3. The initial activation of the *nodal* gene in response to a redox-sensitive b-zip transcription factor (Nam et al., 2007; Range et al., 2007) is not shown. This input acts together with the early, weak ubiquitous input from Univin (U), but as the experiments in Fig. 2B (and many others) indicate, once it gets going, almost all transcriptional activity of the *nodal cis*-regulatory system is due to the feedback input from activated Smad generated by reception of the Nodal signal. The *lefty* gene responds to the same activated Smad input (Su et al., 2009). The Lefty protein is shown interacting both with Nodal protein and with the Alk4 receptor, to form inactive complexes, and both Lefty and Nodal diffuse.

The consequences of the diffusion of Nodal for leveling cell-to-cell Nodal-dependent transcriptional activity are shown in Fig. 4. This

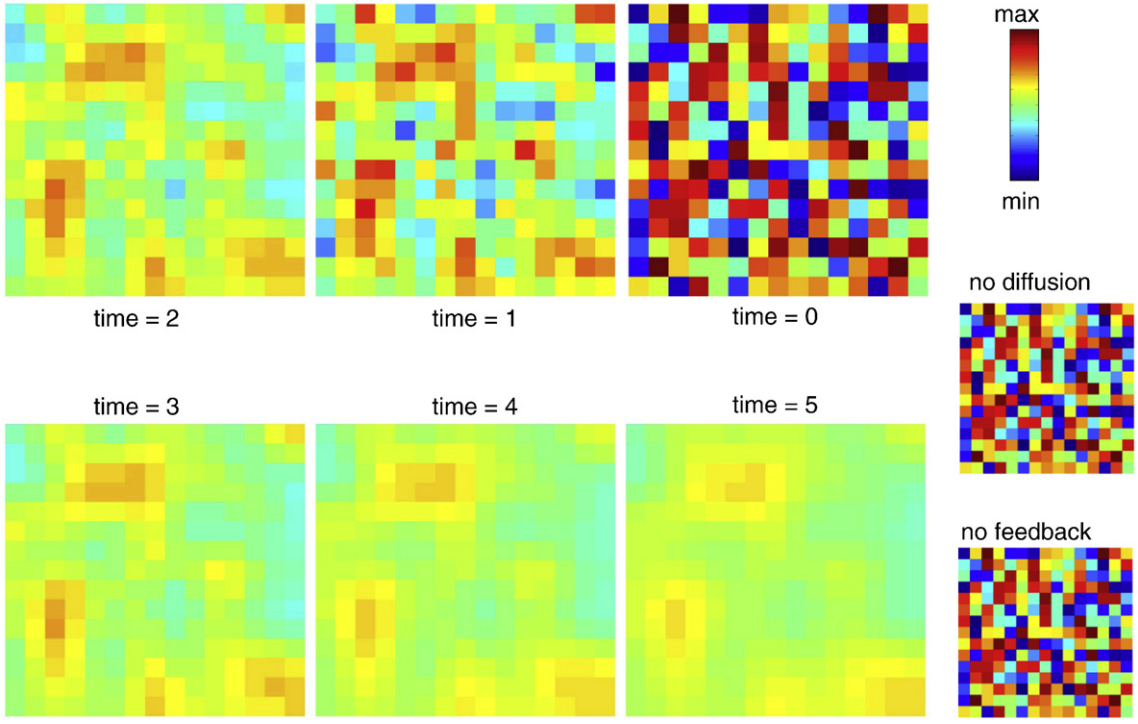

Fig. 4. Illustration of the spatial averaging effect of ligand diffusion. Shown is a 15×15 array of cells (colored squares) within the community effect zone (i.e. where Nodal receptor-binding activity exceeds Lefty activity). The top right panel shows the starting point of the model. For illustrative purposes, each cell in the grid is assigned a random initial *nodal* 'expression level', as indicated by the color bar. The color scale is the same in all four panels. The five panels labeled (time = 1), (time = 2), etc. show five consecutive snap shots of gene expression levels within the array. Nodal in the cell (i,j), where i is the row index and j the column index, is denoted $N_{i,j}(t)$, where t denotes the time point. $N_{i,j}$ at the next time point, i.e. $N_{i,j}(t+1)$, is calculated as: $N_{i,j}(t+1) = \frac{1}{8}\left[4N_{i,j}(t) + N_{i-1,j}(t) + N_{i+1,j}(t) + N_{i,j-1}(t) + N_{i,j+1}(t)\right]$. In the above equation, each cell is assumed to secrete its total synthesized Nodal ligand to the inter-cellular space. Assuming that the vast majority of Nodal ligands do not diffuse beyond the immediate neighbor cells (Yaguchi et al., 2007), the Nodal ligands secreted by each cell are exposed to twice the cell-surface area of one cell. Thus, on average half of the ligands secreted by cell (i,j) will bind receptors on its own surface (first term on the right hand side of the equation). The remaining half will be shared equally among the four adjacent neighbors of cell (i,j). These cells, in turn contribute 1/4 of their ligands each to cell (i,j), as indicated by the next four terms on the right hand side of the equation. For simplicity (and without loss of generality), in these simulations the amount of Nodal secreted at any time point is set to be proportional to the amount of Nodal ligand received in the previous time point. This follows directly from the feedback relation of the circuitry in Fig. 3. The outcome of repeated rounds of ligand secretion, sharing and synthesis is to average the expression levels among neighboring cells (i.e., smooth-out differences). Over time, all cells within the community effect zone are driven to express *nodal* at the same level (here the average of their initial values). For comparison, the two panels at the bottom right show the state of the cellular array at (time = 5) if either the ligand sharing process (see equation above) or the feedback link connecting Nodal activity to the amount of Nodal ligand sensed is removed. In both cases, the activity of Nodal in each cell becomes independent of its activity in the host or neighboring cells at previous times. Thus Nodal expression remains constant throughout the simulation.

presents the level of nodal transcription per cell in a "heat map" color scale after successive periods of time, beginning with an extreme initial cell-to-cell variation at the upper right. The rule followed in this calculation is that the intensity (rate) of *nodal* transcription is proportional to the amount of Nodal signal that cell receives, while the amount of Nodal signal it receives is partitioned proportionally to the diffusing contributions of each of the four adjacent cells plus that signal produced by itself which it would bind on a random basis (see caption). The maximally conservative assumption is made that Nodal diffuses only one cell away from its source (were it to diffuse longer distances there would of course be even more intercellular leveling across space). No other components of the mechanism in Fig. 3 are included here, as our only objective is to show that two elemental aspects of this mechanism suffice to cause intercellular leveling of the *nodal* transcription rate: these aspects are that the Nodal ligand outside each cell will diffuse (irrespective of rate of diffusion, which for the minute intercellular distances is not determinant of the outcome); and that the rate of *nodal* gene transcription depends directly on the input from Nodal signal transduction. As time goes on, the variations among the cells disappear, and the level of *nodal* transcription in each cell approaches a common value. So of course would the transcription of the other genes downstream of Nodal generated activated Smad. As the figure shows, if there is no diffusion or no relation between the signal input and the nodal transcription rate in the model, there is no intercellular leveling. While this is an elementarily simple model, its assumptions are likely to differ from reality only in micro-geometric variations that will even out across the field. What Fig. 4 means is that the community effect plausibly enforces uniformity in intensity of expression of regulatory state (see also Bolouri and Davidson, 2002). For simplicity, in all the remaining simulations in this paper, we assume all cells start with equal levels of Nodal activity. In that case, all cells behave identically so that the behavior of one cell is representative of all cells. Also, inside the community effect zone, the numbers of Nodal and Lefty molecules that diffuse out of and away from any given cell will be exactly equal to the numbers of Nodal and Lefty molecules that arrive at that cell's surface from other cells. As a result, we can model the behavior of any single cell within the community effect zone without explicitly modeling diffusion among cells.

Fig. 5A shows the model built to see if Lefty could plausibly be the source of the implied negative feedback, given the approximate values of the parameters established by the model curve fits to the data, shown in Figs. 5B–D. The equations of Fig. 5A are drawn directly from the interaction diagram of Fig. 3. The first three equations describe the dynamics of the complexes between Lefty and Alk4, Lefty and Nodal, and Nodal and Alk4 respectively (see legend). The second three equations give the stoichiometric conservations of Alk4, Nodal, and Lefty. The last four equations give the synthesis and turnover dynamics for *nodal* mRNA, Nodal protein, *lefty* mRNA and Lefty protein respectively (total Alk4 is expected to remain essentially constant, as shown below). All the parameters used in the following are listed in Table S1. In Fig. 5B QPCR measurements for *alk4* mRNA are shown to fit

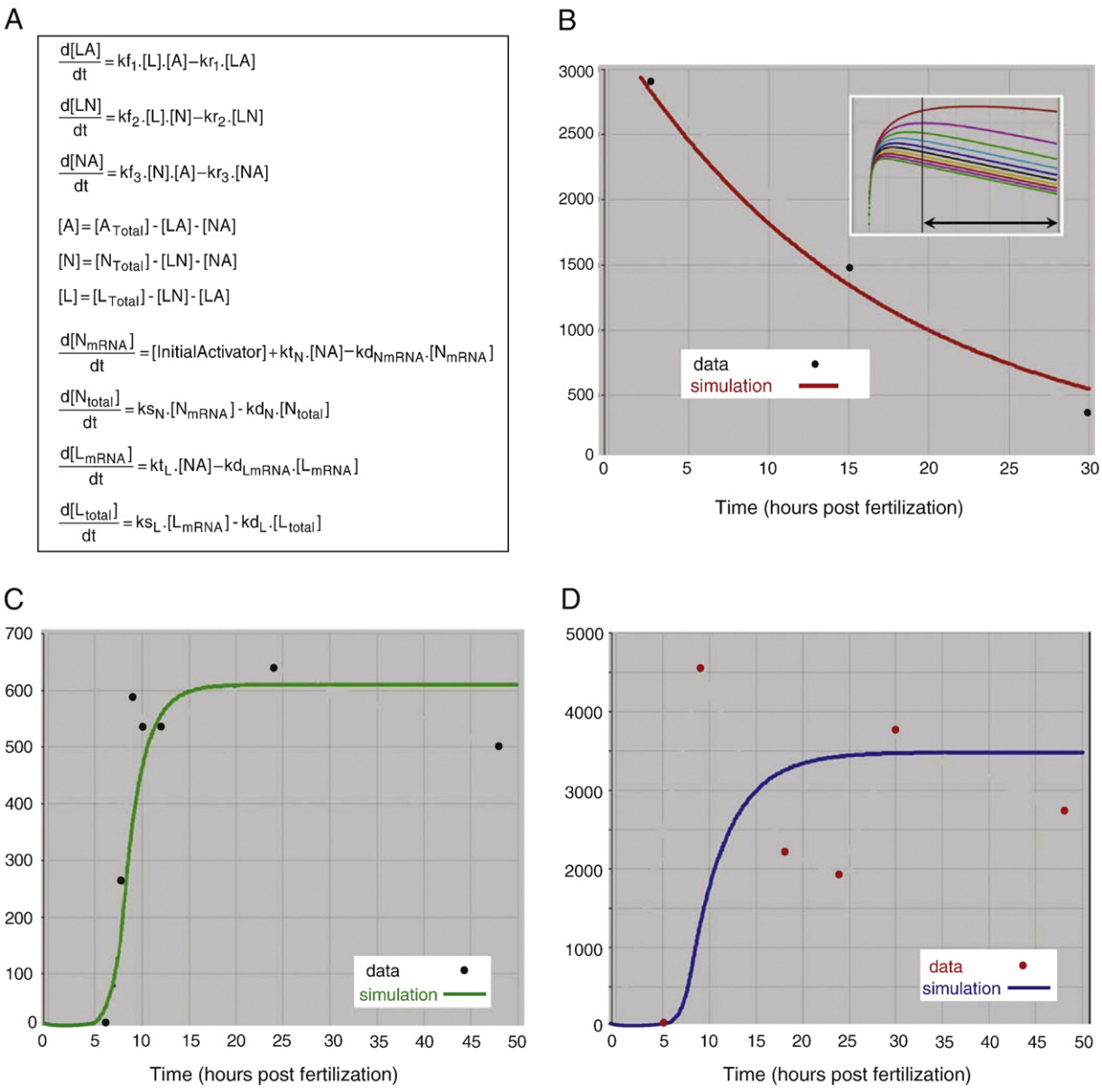

Fig. 5. Model, and model simulations of the Nodal–Lefty community effect. (A) Model. The three Ordinary Differential equations (ODEs) at the top model the interactions of Lefty (L) and Nodal (N) ligands with the Alk4 receptors (A), and with each other. Each interaction is modeled as a first-order reaction. The forward and reverse parameters (kf_i, kr_i, $i = 1,2,3$) were selected such that moderate amounts of Lefty protein can down-regulate but not completely abrogate Nodal:Alk4 binding (all $kf_i = 0.001$ per hour per molecule, and all $kr_i = 0.000005$ per hour). Square brackets denote concentration. LA, Lefty:Alk4 dimer. LN, Lefty:Nodal dimer. NA, Nodal:Alk4 dimer. The following three algebraic equations model the mass-conservation relationships for total Alk4 (A_{total}), total Nodal (N_{total}), and total Lefty (L_{total}). A, N, and L denote free (unbound) Alk4, Nodal and Lefty protein. The last four ODEs model the mRNA and total protein levels of Nodal (N_{mRNA} and N_{total}) and Lefty (L_{mRNA} and L_{total}). Initial *nodal* transcription is assumed to be driven by a ubiquitous activator plus a redox-sensitive input on the oral side, causing initial transcription of the *nodal* gene at a low level (inputs together denoted "initial activator"). Intercellular autoregulatory feedback transcriptional activation of *Nodal* via Alk4 signaling is modeled as a linear function of Nodal:Alk4 dimer concentration ([NA]). A linear activation model is appropriate because, as shown previously (Bolouri and Davidson, 2003), gene activity in the sea urchin embryo occurs on timescales much shorter than that needed to reach steady state. The Nodal:Alk4 driven transcription rates for both genes (kt_N, kt_L) were curve fitted to match measured mRNA levels at steady state (see C and D). Parameters: For both Nodal and Lefty, the rate of protein synthesis is proportional to mRNA concentration, with the proportionality constant set to two protein molecules per minute per mRNA molecule (data for sea urchin embryos reviewed by Davidson, 1986). The mRNA degradation rates ($kd_{NmRNA} = 0.5$ and $kd_{LmRNA} = 0.25$ per hour) are based on the observations of Nam et al. (2007). The protein degradation terms lump together all protein degradation and also the diffusion of protein out of the Nodal community effect region. Lefty is known to diffuse faster than Nodal, therefore kd_L was set to be larger than kd_N. Alk4 receptor concentrations were set to a constant value of 100,000 molecules per cell, for reasons that follow. (B) Decay of Alk4 mRNA. The data show that Alk4 mRNA concentration appears to be undergoing a first-order degradation process throughout the period of interest. The inset shows simulations of Alk4 protein levels using the Alk4 mRNA curve as input. Curves for Alk4 protein half lives ranging from 0.5 h to 10 h (a biologically plausible range given the data of Howard-Ashby et al., 2006). As shown, the level of Alk4 protein remains fairly constant throughout the period of interest (10–30 h, marked by the double-ended arrow). The median value of Alk4 protein is ~100,000 molecules, which was used for the remainder of the simulations. Apart from Alk4, initial concentrations of all other molecules were set to zero. (C) Simulated and measured Nodal mRNA levels over time. (D) Simulated and measured Lefty mRNA levels over time. The model replicates the underlying trend in both data sets. All simulations and parameter fittings were carried out using the freely available version of the Berkeley Madonna modeling environment (http://www.berkeleymadonna.com/), except for the simulations presented in Fig. 4, which were performed with Matlab (http://www.mathworks.com/).

very well to a simple first-order decay. The inset shows that irrespective of the Alk4 protein turnover assumed, using the model simulation tool (see legend), the total amount of Alk4 protein does not vary very much over time. We chose a median value of 100,000 molecules per embryo as a constant value for the Alk4 receptor and kept it constant for the remainder of the exercise. We next determined the approximate rates of *nodal* gene expression, of *nodal* mRNA turnover, and the steady state value of *nodal* mRNA by fitting QPCR

measurements of *nodal* mRNA accumulation (Nam et al., 2007) to the model, as shown in Fig. 5C. There are about 600 molecules of *nodal* mRNA per embryo at steady state. This level is attained over several hours, following activation of the gene at 6–7 h, which means that even under conditions when the positive feedback is operating the absolute rate of transcription per active cell is quite leisurely, only a few percent of the maximal transcription rate possible in sea urchin embryos (for consideration of maximum possible rate, Bolouri and Davidson, 2003). The accumulation curve furthermore shows clearly that the content of *nodal* transcript does not increase after about 15 h. In Fig. 5D a similar fit for *lefty* mRNA is shown. Though this dataset is very noisy it is obvious that there is >5× more *lefty* mRNA per embryo at steady state as there is of *nodal* mRNA. These values are very insensitive to assumptions regarding the exact onset time of the initial pre-feedback activation of the *nodal* gene (Fig. S1), or to the relative magnitude of the initial activation level (Fig. S2). Nor does the magnitude of the initial activation materially affect the steady state levels of either *nodal* or *lefty* mRNA (Fig. S3). The model predicts that the steady state levels are in fact directly proportional to the amount of Alk4 receptor, as might be intuitively supposed (Fig. S4).

The model produces and explains results that have been qualitatively observed in many different experiments. For example,

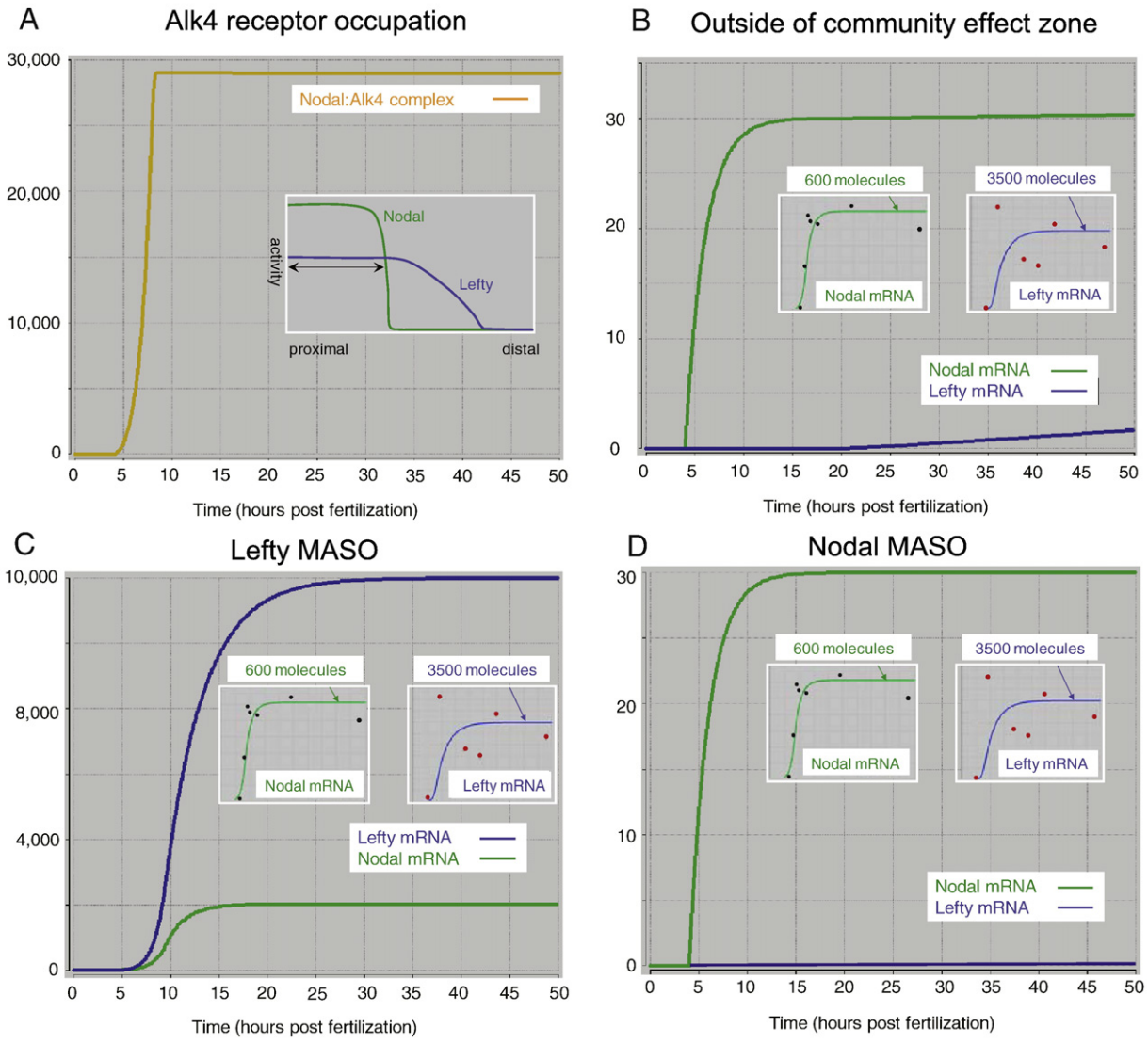

Fig. 6. In silico experiments replicate experimental observations. (A) Formation of steady state amount of Nodal–Alk4 complex due to Lefty competition for Nodal. The simulation shows that Lefty competition quickly reduces the abundance of Nodal:Alk4 complexes (within the community effect zone) to a steady state level far below the maximum possible. Since there are a total of 100,000 Alk4 receptors per simulated cell, in the absence of Lefty, the steady state abundance of Nodal:Alk4 complexes would be 100,000. But within the community effect zone, the steady state abundance of Nodal:Alk4 complexes is only about 1/3 of this maximum, illustrating the partial, inhibitory effect of Lefty on Nodal. In cells immediately outside the community effect zone, Lefty protein activity is stronger than Nodal activity because Lefty diffuses farther than Nodal (inset, double-ended arrow indicates the edge of the region within the community effect zone, in which Nodal activity dominates over Lefty). (B) *lefty* and *nodal* transcript levels just outside the community effect zone. Here the community effect zone is defined as the domain where the *nodal* gene is being expressed (as in Fig. 4), and the domain outside is the region where Lefty protein has diffused beyond the nodal protein domain. The simulation shows how, outside of the community effect zone, *nodal* and *lefty* transcription levels are negligibly small. This is because large numbers of Lefty molecules diffusing in from the community effect zone titrate away both Alk4 receptors and also the small numbers of Nodal molecules diffusing in. As a result, there is no SMAD2/3 mediated transcription of *nodal* in these cells, and since this factor also drives *lefty* transcription, this gene also becomes essentially silent. (C) Simulated effect of lefty MASO. The simulation shows the effect of turning off *lefty* translation within the community effect zone. The effect of such an intervention is to remove the negative feedback of Lefty on Nodal. As a result, the positive Nodal intercellular feedback loop drives the expression levels of both *nodal* and *lefty* to saturation levels (approximately three-fold higher than for unperturbed cells, shown in the inset). (D) Simulated effect of Nodal MASO. The simulation shows the effect of turning off Nodal translation. As expected, in the absence of Nodal protein, *lefty* transcription is nonexistent (Lefty mRNA levels are zero throughout the simulation). With no Lefty protein, there is no negative feedback on Nodal. However, in contrast to (6C), here the Nodal positive feedback loop remains inactive because there is no Nodal protein being synthesized. As a result, Nodal mRNA levels remain at the basal levels driven by the initial activators (about 20-fold less than in unperturbed cells (inset)).

Duboc et al. (2008) concluded that Lefty diffusion beyond the domain of Nodal presence restricts the oral field by setting up a boundary beyond which there is no Nodal activity. Fig. 6A shows first of all that within the community effect domain, i.e., the oral ectoderm, it is indeed Lefty that restricts the steady state level of Nodal to about one-third of the saturation maximum, which we have seen would be equal to the number of Alk4 receptors, here about 100,000. The cartoon in the inset of Fig. 6A conveys the very sharp observed fall off in effective Nodal signaling away from the sharply bounded zone of *nodal* transcription (Yaguchi et al, 2007), while across the boundary the freely diffusing Lefty protein declines more slowly as in the arbitrary drawing, though there are no relevant direct measurements. Irrespective of the more distal Lefty levels, across the boundary, as the drawing shows, where there is excess Lefty, Nodal activity is essentially abolished. In Fig. 6B, we see that across the boundary the transcript levels for *nodal* mRNA have fallen to only about 5% of their steady state levels within the oral ectoderm, while transcription of *lefty* is close to zero. This result is very insensitive to the absolute amount of Lefty protein, but the sharpness of the boundary depends on the stoichiometry: over a certain amount of Lefty the *nodal* positive feedback loop is abolished and transcription of *nodal* and *lefty* are effectively shut down (Fig. S5). It is very important here to distinguish between the process by which the size and position of the oral ectoderm transcriptional domain are initially established, and the maintenance and sharpness of the boundary. The oral spatial domain of *nodal* transcription is determined by the initial *cis*-regulatory inputs into the *nodal* gene as described (Nam et al, 2007; Range et al., 2007), not by the dynamics of Lefty–Nodal interaction; but the domain is prevented from spreading further and is made abrupt by the Lefty-dependant mechanism Duboc et al. (2008) proposed, as the simulations show.

Duboc et al. (2004, 2008) also studied the effects of treatment with *nodal* and *lefty* MASOs. By WMISH, *lefty* MASO caused gross overexpression of *nodal*, and extension of both *nodal* and *lefty* transcription all around the embryo, and *nodal* MASO caused extinction of lefty expression as well as of other oral ectoderm markers. The simulation in Fig. 6C shows that removal of the input of Lefty protein, as would be caused by *lefty* MASO, in the model indeed results in derepression of *nodal* so that the steady state attained within the oral ectoderm is the level expected when all the Alk4 in the system is occupied by Nodal, i.e., about 3× over normal (inset; see above). Concomitantly, *lefty* mRNA levels are also raised by this amount compared to normal (inset). When nodal MASO effects are simulated, as in Fig. 6D, the result is to decrease transcription of the *nodal* gene by 95% because of loss of the feedback effect, and therefore to abolish lefty mRNA. Note that all the simulation results are very insensitive to the parameters chosen for interaction of the proteins Nodal, Alk4 and Lefty with one another; virtually identical curves are obtained for *nodal* and *lefty* mRNAs over a10-fold range of these parameters (Fig. S6A–D).

In sum, in Figs. 5, 6, and S1–6 we have explored the quantitative behavior of a model capturing the network of interactions shown in Fig. 3. We have used parameters for the synthesis dynamics taken off the measured accumulation kinetics for *nodal*, *lefty*, and *alk4* mRNAs, plus a well established translation rate taken from the literature. The remaining parameters for protein interaction were assumed on the basis of reasonable guesses, but the nature of the model output depends hardly at all on these values. The results of this exercise are several. First, the qualitative and intuitive functions proposed to devolve from the interaction network in Fig. 3 and observed at the whole mount in situ level in earlier work do indeed follow from the topology of this network. Second, the community effect may plausibly act both to impose uniformity of gene expression within the domain and produce steady state expression of the regulatory state. Third, in order to do this the feedback wiring of the ligand gene requires a downstream damper, the role played here by Lefty. Since, as we see above, this wiring is widespread for Tgfβ genes, and perhaps for other polypeptide ligand genes as well, the generality of this damper feature is implied as well.

Discussion: evolutionary problems raised by the community effect

A huge number of diverse cell-surface molecules, cadherins, lectins, integrins, and many others, contribute to intercell communication in architectural tissues, many functioning as ligands which interact with specific cell-surface receptors (for review see, Hynes and Zhao (2000); Whittaker et al. (2006)). The latter either have or are intimately associated with intracellular domains, capable of indirectly altering intracellular state in multiple ways and at multiple levels. Why then would ligands belonging to signaling families used over and over again in development for inductive signaling also have been co-opted to the intra-domanic community effect function?

The signaling systems used for inductive developmental functions all basically operate in a similar manner: the immediate early response factor that signal reception alters is always a transcriptional regulatory factor or cofactor operating in the nucleus, and its direct targets always include the *cis*-regulatory systems of regulatory genes. Signal driven expression of regulatory genes is a developmentally powerful change, as it constitutes alteration of the regulatory state; hence the powerful developmental phenomenon of inductive signaling. The use of the same signaling systems within territorial developmental domains in the community effect can thus be regarded as deployment of an upper echelon control device, which directly affects that which controls all else: the regulatory state. What happens as a result of deploying this high level control feature is different from what happens in inductive signaling: as we show in our model, the community effect functions to impose uniformity of regulatory state and to set quantitatively the level of expression of the regulatory state. But it has in common with inductive signaling that it operates at the top of the hierarchical control apparatus, directly at the level where the regulatory state is generated. The cataclysmic consequences of interruption of the oral ectoderm community effect by interference with *nodal* or *lefty* mRNA translation (Duboc et al., 2004, 2008; Su et al., 2009; and above) can only be generally understood by reference to the principle that the community effect operates at the top of the regulatory gene network hierarchy.

An aspect of community effect function we have not explicitly touched on is that it is another in the growing category of gene regulatory network devices which act to ensure reliability, reproducibility, temporal stability, irreversibility of developmental decisions. We have noted before (Oliveri and Davidson, 2007) that developmental gene regulatory networks have evolved to consist of an overlay of multiple subnetworks, all contributing to and ensuring the right outcome. Examples are double negative gates (Davidson and Levine, 2008) which not only impose the right pattern of gene expression in the right place but also actively prevent it in the wrong place; the logic "toggle switches" common to inductive signaling which both stimulate expression of given regulatory genes in target cells while also repressing the same genes in all other cells (Barolo and Posakony, 2002; Ransick and Davidson, 2006; Istrail and Davidson, 2005); regulatory state "exclusion functions" which specifically repress key regulatory genes that must be expressed in alternative regulatory states (Oliveri and Davidson, 2007). These devices are not redundantly wired into gene regulatory networks as shown immediately by the disasters that occur when the operation of any of them is interrupted. Suffice it to say that at least superficially, it would seem that regulatory systems causing similar developmental progressions could be designed without using all the apparatus that we see revealed in the actual network topologies of animal development (an experimental challenge for the synthetic developmental biology of the future). But in fact, non-parsimonious designs are what evolution has produced, though in any given subcircuit they appear always elegant. The explanation, in addition to the overused argument that

"robustness" must be good, is in fact likely to be that the subcircuits have been loaded in to the system at different times in evolution: in other words, as gene networks have become more baroque development of each clade has become more secure. Thus the reason that all surviving subcircuits are necessary is simply that any redundant linkages would have decayed away. Perhaps if we could compare evolutionary stem group and crown group gene regulatory networks we would see exactly this kind of difference, which might suggest why crown groups are more stable.

The community effect is likely not to be primitive, but rather a derived type of signal ligand gene wiring. Perhaps the earliest developmental metazoan signaling functions were inductive; multiple signaling systems are utilized even in the single celled choanaflagellate sister group to the metazoans (King et al., 2003) where they must be used to induce changes in cell function in response to environmental information, as in other single cell organisms. But community effect wiring of signal ligand genes is a feature that has apparently been re-invented many times. Direct autoregulation is very common in genes encoding transcription factors. What it requires is simply appearance in a *cis*-regulatory module of target sites for the factor encoded by the gene. Its utility is obvious, as in development, inputs that initially alter gene expression are often transient, and positive autoregulation is a state stabilization device. Very similarly, the indirect feedback wiring of the community effect also just requires appearance of target sites in a *cis*-regulatory module of the ligand gene, here for the immediate early response transcription factor. As we see explicitly in the case of *nodal*, the consequence is much the same as in regulatory gene autoregulation: not only does the expression increase in intensity but it essentially becomes independent of the initial activating inputs, again a state stabilization device. But evolutionary appearance of community effect wiring might have had many different useful effects in addition, such as potentiating geometrically larger and larger fields of similarly behaving cells. Like many other biological functions community effect wiring is also intrinsically dangerous, a potential mechanism for a given domanic regulatory state to take over globally, just as occurs in a *lefty* MASO treated sea urchin embryo. Some kind of negative feedback somewhere in the system is a necessary safeguard. In our sea urchin case it is one that operates outside the cell. Thus a general prerequisite for the evolutionary appearance of community effect wiring is likely to have been the pre-existence of damping mechanisms affecting either the transcription, signal transduction, or extracellular functionality of the signal transmission.

Acknowledgments

This research was supported by NIH grant GM-61005. We are grateful to our colleagues Smadar Ben Tabou de-Leon and Jongmin Nam for very helpful suggestions on a draft of the manuscript.

Appendix A. Supplementary data

Supplementary data associated with this article can be found, in the online version, at doi:10.1016/j.ydbio.2009.06.007.

References

Barolo, S., Posakony, J.W., 2002. Three habits of highly effective signaling pathways: principles of transcriptional control by developmental cell signaling. Genes Dev. 16, 1167–1181.

Bauer, H., Lele, Z., Rauch, G.-J., Geisler, R., Hammerschmidt, M., 2001. The type I serine/threonine kinase receptor Alk8/Lost-a-fin is required for Bmp2b/7 signal transduction during dorsoventral patterning of the zebrafish embryo. Development 128, 849–858.

Bolouri, H., Davidson, E.H., 2002. Modeling transcriptional regulatory networks. BioEssays 24, 1118–1129.

Bolouri, H., Davidson, E.H., 2003. Transcriptional regulatory cascades in development: initial rates, not steady state, determine network kinetics. Proc. Natl. Acad. Sci. U. S. A. 100, 9371–9376.

Cameron, R.A., Fraser, S.E., Britten, R.J., Davidson, E.H., 1990. Segregation of oral from aboral ectoderm precursors is completed at 5th cleavage in the embryogenesis of *Strongylocentrotus purpuratus*. Dev. Biol. 137, 77–85.

Cao, Y., Knöchel, S., Oswald, F., Donow, C., Zhao, H., Knöchel, W., 2006. XBP1 forms a regulatory loop with BMP-4 and suppresses mesodermal and neural differentiation in *Xenopus* embryos. Mech. Dev. 123, 84–96.

Chanut, F., Heberlein, U., 1997. Role of *decapentaplegic* in initiation and progression of the morphogenetic furrow in the developing *Drosophila* retina. Development 124, 559–567.

Chen, C., Shen, M.M., 2004. Two modes by which Lefty proteins inhibit nodal signaling. Curr. Biol. 14, 618–624.

Cheng, S.K., Olale, F., Brivanlou, A.H., Schier, A.F., 2004. Lefty blocks a subset of TGFβ signals by antagonizing EGF-CFC coreceptors. PLos Biol. 2, 0215.

Clayton, D.F., Darnell Jr, J.E., 1983. Changes in liver-specific compared to common gene transcription during primary culture of mouse hepatocytes. Mol. Cell. Biol. 3, 1552–1561.

Clayton, D.F., Harrelson, A.L., Darnell Jr, J.E., 1985. Dependence of liver-specific transcription on tissue organization. Mol. Cell. Biol. 5, 2623–2632.

Coffman, J.A., Davidson, E.H., 2001. Oral–aboral axis specification in the sea urchin embryo. I. Axis entrainment by respiratory asymmetry. Dev. Biol. 230, 18–28.

Coffman, J.A., McCarthy, J.J., Dickey-Sims, C., Robertson, A.J., 2004. Oral–aboral axis specification in the sea urchin embryo II. Mitochondrial distribution and redox state contribute to establishing polarity in *Strongylocentrotus purpuratus*. Dev. Biol. 273, 160–171.

Davidson, E.H., 1986. Gene Activity in Early Development, Third Edition. Academic Press, Orlando, FL.

Davidson, E.H, 2006. The regulatory genome. Gene Regulatory Networks in Development and Evolution. Academic Press/Elsevier, San Diego.

Davidson, E.H., Levine, M., 2008. Properties of developmental gene regulatory networks. Proc. Natl. Acad. Sci. U. S. A. 105, 20063–20066.

Duboc, V., Röttinger, E., Besnardeau, L, Lepage, T., 2004. Nodal and BMP2/4 signaling organizes the oral–aboral axis of the sea urchin embryo. Dev. Cell. 6, 397–410.

Duboc, V., Lapraz, F., Besnardeau, L., Lepage, T., 2008. Lefty acts as an essential modulator of Nodal activity during sea urchin oral–aboral axis formation. Dev. Cell 6, 397–410.

Flowers, V.L., Courteau, G.R., Poustka, A.J., Weng, W., Venuti, J.M., 2004. Nodal/activin signaling establishes oral–aboral polarity in the early sea urchin embryo. Dev. Dyn. 231, 727–740.

Gurdon, J.B., 1988. A community effect in animal development. Nature 336, 772–774.

Hepker, J., Blackman, R.K., Holmgren, R., 1999. Cubitus interruptus is necessary but not sufficient for direct activation of a wing-specific *decapentaplegic* enhancer. Development 126, 3669–3677.

Hild, M., Dick, A., Rauch, G.-J., Meier, A., Bouwmeester, T., Haffer, P., Hammerschmidt, M., 1999. The *smad5* mutation *somitabun* blocks Bmp2b signaling during early dorsoventral patterning of the zebrafish embryo. Development 126, 2149–2159.

Howard-Ashby, M., Materna, S.C., Brown, C.T., Tu, Q., Oliveri, P., Cameron, R.A., Davidson, E.H., 2006. High regulatory gene use in sea urchin embryogenesis: implications for bilaterian development and evolution. Dev. Biol. 300, 27–34.

Hursh, D.A., Padgett, R.W., Gelbart, W.M., 1993. Cross regulation of *decapentaplegic* and *Ultrabithorax* transcription in the embryonic visceral mesoderm of *Drosophila*. Development 117, 1211–1222.

Hynes, R.O., Zhao, Q., 2000. The evolution of cell adhesion. J. Cell Biol. 150, F89–F95.

Istrail, S., Davidson, E.H., 2005. Logic functions of the genomic *cis*-regulatory code. Proc. Natl. Acad. Sci. USA 102, 4954–4959.

King, N., Hittinger, C.T., Carroll, S.B., 2003. Evolution of key cell signaling and adhesion protein families predates animal origins. Science 301, 361–363.

Koide, T., Hayata, T., Cho, W.Y., 2005. *Xenopus* as a model system to study transcriptional regulatory networks. Proc. Natl. Acad. Sci. U. S. A. 102, 4943–4948.

Minokawa, T., Wikramanayake, A.H., Davidson, E.H., 2005. *cis*-Regulatory inputs of the *wnt8* gene in the sea urchin endomesoderm network. Dev. Biol. 288, 545–558.

Nam, J., Su, Y.-H., Lee, P.Y., Robertson, A.J., Coffman, J.A., Davidson, E.H., 2007. *Cis*-regulatory control of the *nodal* gene, initiator of the sea urchin oral ectoderm gene network. Dev. Biol. 306, 860–869.

Oliveri, P., Davidson, E.H., 2007. Built to run, not fail. Science 315, 1510–1511.

Range, R., Lapraz, F., Quirin, M., Marro, S., Besnardeau, L., Lepage, T., 2007. *Cis*-regulatory analysis of *nodal* and maternal control of dorsal–ventral axis formation by Univin, a TGF-β related to Vg1. Development 134, 3649–3664.

Ransick, A., Davidson, E.H., 2006. *cis*-Regulatory processing of Notch signaling input to the sea urchin *glial cells missing* gene during mesoderm specification. Dev. Biol. 297, 587–602.

Sakuma, R., Ohnishi, Y., Meno, C., Fujii, H., Juan, H., Takeuchi, J., Ogura, T., Li, E., Miyazono, K., Hamada, H., 2002. Inhibition of Nodal signalling by Lefty mediated through interaction with common receptors and efficient diffusion. Genes Cell. 7, 401–412.

Smith, J., Theodoris, C., Davidson, E.H, 2007. A gene regulatory network subcircuit drives a dynamic pattern of gene expression. Science 318, 794–797.

Staehling-Hampton, K., Hoffmann, F.M., 1994. Ectopic *decapentaplegic* in the *Drosophila* midgut alters the expression of five homeotic genes, *dpp*, and *wingless*, causing specific morphological defects. Dev. Biol. 164, 502–512.

Su, Y.-H., Li, E., Geiss, G.K., Longabaugh, W.J.R., Krämer, A., Davidson, E.H., 2009. A perturbation model of the gene regulatory network for oral and aboral ectoderm specification in the sea urchin embryo. Dev. Biol. 329, 410–421.

Whittaker, C.A., Befgeron, K.F., Whittle, J., Brandhorst, B.P., Burke, R.D., Hynes, R.O., 2006. The echinoderm adhesome. Dev. Biol. 300, 252–266.

Yaguchi, S., Yaguchi, J., Burke, R.D., 2007. Sp-Smad2/3 mediates patterning of neurogenic ectoderm by nodal in the sea urchin embryo. Dev. Biol. 302, 494–503.